

Optimization of Reconfigurable Intelligent Surfaces with Electromagnetic Field Exposure Constraints

A. Zappone, *Senior Member, IEEE* and M. Di Renzo, *Fellow, IEEE*

Abstract—This work tackles the problem of maximizing the achievable rate in a reconfigurable intelligent surface (RIS)-assisted communication link, by enforcing conventional maximum power constraints and additional constraints on the maximum exposure to electromagnetic radiations of the end-users. The RIS phase shift matrix, the transmit beamforming filter, and the linear receive filter are jointly optimized, and two provably convergent and low-complexity algorithms are developed. One algorithm can be applied to general system setups, but does not guarantee global optimality. The other is shown to be provably optimal in the special case of isotropic electromagnetic exposure constraints. The numerical results show that RIS-assisted communications can ensure high data rate transmissions while guaranteeing users' exposure constraints to radio frequency emissions.

I. INTRODUCTION

With fifth generation (5G) networks being rolled out, the attention of the research community is shifting towards the next generation of wireless networks. Among the candidate technologies for sixth generation (6G) networks, the paradigm of programmable smart radio environments based on the use of reconfigurable intelligent surfaces (RISs) is emerging as a way of ensuring high data rates, high energy efficiency, and a high degree of flexibility to adapt to sudden and heterogeneous service requests [1], [2], [3]. Environmental objects separating the endpoints of a communication link can be coated with RISs, which can be dynamically reconfigured so as to provide channel customization features. In the area of resource allocation for RIS-assisted networks, most research contributions are focused on the maximization of the network rate [4], [5], on the minimization of the network consumed power [6], or on the maximization of the global energy efficiency [4], [7].

At the same time, a relevant issue for future wireless networks is the growing concerns for electromagnetic pollution. Although, at present, non-ionizing radio frequency radiations have not been associated to any health condition [8], the continuous exposure to electromagnetic fields (EMF) is a factor that raises concerns among end-users and diminishes their acceptance of emerging transmission technologies and massive network deployments [9]. A few studies have appeared in the literature to investigate resource allocation schemes that minimize the EMF exposure of human users. In [10], a survey on reducing the electromagnetic radiation in wireless systems is provided. In [11], a method for evaluating the specific absorption rate (SAR) of multi-antenna systems is proposed and evaluated. In [12], the EMF exposure in orthogonal frequency-division multiplexing (OFDM) systems is minimized subject to minimum rate requirements for the users, and the authors of

[13] have recently designed transmit policies that dynamically allocate users' electromagnetic radiation exposure over time.

While all these previous works considered the problem of EMF-aware communications in legacy wireless systems, an EMF-aware scheme for RIS-based wireless networks has recently been developed in [14]. Therein, the users' electromagnetic exposure is minimized subject to quality of service constraints. In this work, on the other hand, we consider the different problem of maximizing the achievable rate in an RIS-assisted communication link, enforcing both maximum power constraints and maximum EMF exposure constraints. The optimization problem is tackled with respect to the RIS phase shift matrix, the transmit beamforming filter, and the linear receive filter. In particular, the EMF constraints are formulated in terms of maximum acceptable values for the SAR, which is a measure of the rate at which the electromagnetic energy is absorbed per unit mass by a human body when it is exposed to a radio frequency electromagnetic field [11], [13].

In particular, we devise two provably convergent optimization algorithms for EMF-aware RIS-assisted communications. The first algorithm is based on the use of alternating maximization and has a complexity that is linear in the number of RIS elements and polynomial in the number of transmit and receive antennas. The second algorithm achieves global optimality in the notable special case of isotropic EMF exposure constraints, and has a complexity that is linear in the number of RIS elements and in the number of transmit and receive antennas. The numerical results show that RIS-assisted communications ensure high data rate transmissions while guaranteeing users' exposure constraints to radio frequency emissions.

II. SYSTEM MODEL

We consider a single-user system in which a transmitter equipped with N_T antennas and a receiver equipped with N_R antennas communicate through an RIS. The direct link between the transmitter and receiver is assumed to be weak enough to be ignored. We denote by δ the end-to-end path loss, by \mathbf{H} and \mathbf{G} the fading channels from the transmitter to the RIS and from the RIS to the receiver, respectively, by \mathbf{q} the unit-norm transmit beamformer, and by \mathbf{w} the unit-norm receive combiner.

The RIS is made of N elementary passive scatterers, which can be individually and locally optimized, and can independently reflect the radio wave impinging upon them according to a unit amplitude reflection coefficient $e^{j\phi_n}$, with $n = 1, \dots, N$ and j denoting the imaginary unit. For ease of notation, we introduce the $N \times 1$ vectors $\mathbf{h} = \mathbf{H}\mathbf{q}$, with components $[h_1, \dots, h_N]$, $\mathbf{g} = \mathbf{w}^H \mathbf{G}$, with components $[g_1, \dots, g_N]$, and the $N \times N$ diagonal matrix $\mathbf{\Gamma} = \text{diag}(e^{j\phi_1}, \dots, e^{j\phi_N})$, where $(\cdot)^H$ is the Hermitian operator.

A. Zappone is with the University of Cassino and Southern Lazio, 03043 Cassino, Italy (alessio.zappone@unicas.it). M. Di Renzo is with Université Paris-Saclay, CNRS, CentraleSupélec, Laboratoire des Signaux et Systèmes, 91192 Gif-sur-Yvette, France (marco.di-renzo@universite-paris-saclay.fr).

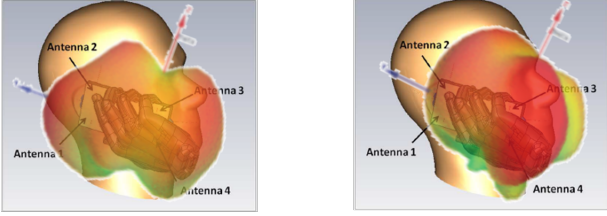


Fig. 1. Example of EMF exposure for two beamforming vectors.

We assume that a reliable channel estimation phase has been performed, and that the RIS phase configuration can be set by sending a configuration signal to an RIS controller with minimal signal processing, transmission/reception, and power storage capabilities [1, Fig. 4]. Further information on the impact of channel estimation overhead and RIS configuration can be found in [4]. Under these assumptions, the system achievable rate is expressed as

$$R = B \log_2 \left(1 + \frac{P}{\delta \sigma^2} |\mathbf{w}^H \mathbf{G} \Phi \mathbf{H} \mathbf{q}|^2 \right), \quad (1)$$

with p being the transmit power, B the communication bandwidth, and σ^2 the receive noise power.

A. EMF-Aware Optimization: Near-Field SAR Constraints

Portable wireless devices, e.g., mobile phones, tablets, provide connectivity by integrating multiple antennas that can be activated simultaneously. The human body in close proximity to these devices absorbs some of the electromagnetic radiation, as illustrated in Fig. 1 for a multi-antenna handset. Each device is required to comply with specific SAR limits of radiation that are considered safe for the body [13]. The challenge of fulfilling SAR compliance is exacerbated by the existence of multiple transmit antennas in portable wireless devices, which usually increase the maximum potential exposure for a given total transmit power. As discussed in [11] and sketched in Fig. 1, multiple transmit antennas cause large near-field SAR variations, due to the combinations of the precoding gains and phases across the antennas, which have significant impact on the far-field performance of multi-antenna wireless systems.

Motivated by these considerations, the objective of this paper is to maximize the rate in (1) subject to both power and EMF constraints, as a function of the RIS phase shift matrix Φ , the beamforming vector \mathbf{q} , and the receive filter \mathbf{w} . The main goal of this paper is, in particular, to assess the possibility of using RISs for enhancing the data rate of legacy wireless systems while reducing the EMF exposure of the users.

To this end, we formulate the following problem

$$\max_{\Phi, \mathbf{q}, \mathbf{w}} |\mathbf{w}^H \mathbf{G} \Phi \mathbf{H} \mathbf{q}| \quad (2a)$$

$$\text{s.t. } \phi_n \in [0, 2\pi] \quad (2b)$$

$$\sum_{n=1}^{N_T} c_n |q_n| \leq P_q, \quad \sum_{n=1}^{N_T} |q_n|^2 \leq 1 \quad (2c)$$

$$\sum_{n=1}^{N_R} d_n |w_n| \leq P_w, \quad \sum_{n=1}^{N_R} |w_n|^2 \leq 1, \quad (2d)$$

wherein P_q and P_w are the maximum EMF constraints at the transmitter and receiver side, respectively, while $\{c_n\}_{n=1}^{N_T}$ and

$\{d_n\}_{n=1}^{N_R}$ are the EMF absorption coefficients, which account for the magnitude of the total electric field absorbed by the human body due to the beamformer applied by the n -th transmit antenna, with $n = 1, \dots, N_T$, and due to the receive combiner applied by the n -th receive antenna, with $n = 1, \dots, N_R$. It is worth noting that the EMF constraint does not apply to the RIS because of the unit modulus design assumption of the matrix of reflection coefficients.

III. SUM-RATE MAXIMIZATION

To tackle the non-convex problem in (2), two methods are developed. The former is based on alternating optimization, while the latter derives the problem global solution in closed-form in a notable special case.

A. Maximization by Alternating Optimization

Problem (2) can be tackled by means of alternating optimization with respect to the RIS phase shift matrix Φ , the beamforming vector \mathbf{q} , and the receive filter \mathbf{w} .

1) *Optimization of Φ* : When \mathbf{q} and \mathbf{w} are fixed, the problem with respect to Φ becomes

$$\max_{\Phi} |\mathbf{w}^H \mathbf{G} \Phi \mathbf{H} \mathbf{q}| \quad (3a)$$

$$\text{s.t. } \phi_n \in [0, 2\pi]. \quad (3b)$$

Problem (3) is solved by setting $\phi_n = -\angle g_n^* h_n$, where $(\cdot)^*$ is the complex conjugate and g_n, h_n are defined in Sec. II.

2) *Optimization of \mathbf{q}* : When Φ and \mathbf{w} are fixed, the optimization of \mathbf{q} can be cast as

$$\max_{\mathbf{q}} |\mathbf{v}^H \mathbf{q}| \quad (4a)$$

$$\text{s.t. } \sum_{n=1}^{N_T} c_n |q_n| \leq P_q, \quad \sum_{n=1}^{N_T} |q_n|^2 \leq 1, \quad (4b)$$

wherein $\mathbf{v}^H = \mathbf{w}^H \mathbf{G} \Phi \mathbf{H}$, and P_q is the maximum allowed EMF exposure due to the transmit antennas. The constraints in (4b) involve only the moduli of the components of \mathbf{q} . Thus, it is optimal to set the phases of q_n so as to compensate for the phases of the entries v_n^* in \mathbf{v}^H . Plugging $\angle q_n = \angle v_n$ into (4) leaves us with the problem of optimizing the moduli of the entries of \mathbf{q} , which, by setting $x_n = |q_n|$, can be cast as

$$\max_{\mathbf{x}} \sum_{n=1}^{N_T} |v_n| x_n \quad (5a)$$

$$\text{s.t. } \sum_{n=1}^{N_T} c_n x_n \leq P_q \quad (5b)$$

$$\sum_{n=1}^{N_T} x_n^2 \leq 1, \quad x_n \geq 0, \quad \forall n \quad (5c)$$

Problem (5) is convex and can be solved globally with polynomial complexity.

3) *Optimization of \mathbf{w}* : The optimization of \mathbf{w} is formally equivalent to that of \mathbf{q} . Defining $\mathbf{u} = \mathbf{G} \Phi \mathbf{H} \mathbf{q}$ and denoting by P_w the maximum allowed EMF exposure due to the receive antennas, the same line of reasoning used to optimize \mathbf{q} leads

Algorithm 1 Alternating maximization of Problem (2)

 Initialize \mathbf{w} and \mathbf{q} to feasible values.

repeat

 $\mathbf{g} = \mathbf{w}^H \mathbf{G}; \mathbf{h} = \mathbf{H} \mathbf{q}; \phi_n = -\angle g_n^* h_n, \forall n = 1, \dots, N;$
 $\mathbf{v}^H = \mathbf{w}^H \mathbf{G} \Phi \mathbf{H}; q_n = x_n e^{j\angle v_n}, \forall n = 1, \dots, N,$ with \mathbf{x}
 the solution of Problem (5);
 $\mathbf{u} = \mathbf{G} \Phi \mathbf{H} \mathbf{q}; w_n = y_n e^{j\angle u_n}, \forall n = 1, \dots, N,$ with \mathbf{y}
 the solution of Problem (6);

 until Convergence

 us to setting $\angle w_n = \angle u_n$, and to optimizing the moduli of the components of \mathbf{w} by solving the optimization problem

$$\max_{\mathbf{y}} \sum_{n=1}^{N_R} |u_n| y_n \quad (6a)$$

$$\text{s.t.} \sum_{n=1}^{N_R} d_n y_n \leq P_w \quad (6b)$$

$$\sum_{n=1}^{N_R} y_n^2 \leq 1, y_n \geq 0, \forall n \quad (6c)$$

 where we have set $y_n = |w_n|$ for $n = 1, \dots, N$. Similar to Problem (5), Problem (6) is convex and thus can be globally solved with polynomial complexity.

 The overall optimization algorithm can be stated as in Algorithm 1, which monotonically increases the value of the objective of (2) and, thus, is convergent. The computational complexity of each iteration of Algorithm 1 is linear in N , since $\phi_n = -\angle g_n^* h_n$ needs to be computed N times, and is polynomial in N_T and N_R , due to the convexity of Problem (5) and Problem (6). Finally, the complexity of Algorithm 1 scales with the total number of iterations until convergence.

B. Isotropic EMF Constraints

 Let us now consider the special case in which $c_n = c$ for $n = 1, \dots, N_T$ and $d_n = d$ for $n = 1, \dots, N_R$. This case study is of practical relevance because it is likely that, for typical co-located multi-antenna devices, the human body has the same SAR for every antenna of the array.

In this case, Problem (2) can be rewritten as

$$\max_{\Phi, \mathbf{q}, \mathbf{w}} |\mathbf{w}^H \mathbf{G} \Phi \mathbf{H} \mathbf{q}| \quad (7a)$$

$$\text{s.t.} \phi_n \in [0, 2\pi] \quad (7b)$$

$$\sum_{n=1}^{N_T} |q_n| \leq P_q/c, \sum_{n=1}^{N_T} |q_n|^2 \leq 1 \quad (7c)$$

$$\sum_{n=1}^{N_R} |w_n| \leq P_w/d, \sum_{n=1}^{N_R} |w_n|^2 \leq 1. \quad (7d)$$

 For generic values of the ratios P_q/c and P_w/d , Problem (7) can be tackled by utilizing the same methods developed in Section III. However, it is possible to further simplify Problem (7) when the conditions $P_q/c \leq 1$ and $P_w/d \leq 1$ hold. It is worth noting that this latter setup is of special importance in the context of the EMF-aware design of multi-antenna wireless systems, since the impact of the near-field SAR constraints determines the far-field performance of wireless systems. This is further detailed next, where we also show, in particular, how to obtain the global solution of Problem (7).

 The main enabler to simplify Problem (7) when $P_q/c \leq 1$ and $P_w/d \leq 1$ is to note that the unit-norm constraints can be relaxed without loss of optimality, since they are implied

 by the EMF constraints. To see this, we first observe that, if $P_q/c \leq 1$ and $P_w/d \leq 1$, the following inequalities hold

$$\sum_{n=1}^{N_T} |q_n|^2 \leq \sum_{n=1}^{N_T} |q_n|, \quad (8)$$

$$\sum_{n=1}^{N_R} |w_n|^2 \leq \sum_{n=1}^{N_R} |w_n|, \quad (9)$$

 because the EMF constraints require that $|q_n| \leq 1$ and $|w_n| \leq 1$ for all n when $P_q/c \leq 1$ and $P_w/d \leq 1$.

 Then, if $P_q/c \leq 1$ and $P_w/d \leq 1$, Problem (7) becomes

$$\max_{\Phi, \mathbf{q}, \mathbf{w}} |\mathbf{w}^H \mathbf{G} \Phi \mathbf{H} \mathbf{q}| \quad (10a)$$

$$\text{s.t.} \phi_n \in [0, 2\pi] \quad (10b)$$

$$\sum_{n=1}^{N_T} |q_n| \leq P_q/c, \sum_{n=1}^{N_R} |w_n| \leq P_w/d. \quad (10c)$$

 In Problem (10), the optimization of Φ can be performed as in Section III-A1, while the optimal \mathbf{q} and \mathbf{w} can be obtained in closed-form as described in the next two subsections.

 1) *Optimization of \mathbf{q}* : Defining $\mathbf{v}^H = \mathbf{w}^H \mathbf{G} \Phi \mathbf{H}$ and noting that the optimal phases of the entries of \mathbf{q} need to fulfill the identity $\angle q_n = \angle v_n$, the problem to be solved reduces to

$$\max_{\mathbf{x}} \sum_{n=1}^{N_T} |v_n| x_n \quad (11a)$$

$$\text{s.t.} \sum_{n=1}^{N_T} x_n \leq P_q/c, x_n \geq 0, \forall n \quad (11b)$$

 with $x_n = |q_n|$ for $n = 1, \dots, N_T$. The following result holds.

Proposition 1: Denote by $n_q \in \{1, 2, \dots, N_T\}$ the index such that $|v_{n_q}| \geq |v_n|$, for $n = 1, \dots, N_T$. Then, the optimal solution of Problem (11) is given by

$$\begin{cases} x_n = \frac{P_q}{c}, & \text{for } n = n_q \\ x_n = 0, & \text{for } n \neq n_q \end{cases} \quad (12)$$

Proof: Since $|v_{n_q}| \geq |v_n|$ for $n = 1, \dots, N_T$, there exist non-negative values $\epsilon_1, \dots, \epsilon_{N_T}$ such that $|v_n| = |v_{n_q}| - \epsilon_n$, for $n = 1, \dots, N_T$. Then, the objective (11a) is upper-bounded as

$$\begin{aligned} \sum_{n=1}^{N_T} |v_n| x_n &= |v_{n_q}| x_{n_q} + \sum_{n \neq n_q}^{N_T} (|v_{n_q}| - \epsilon_n) x_n \\ &= |v_{n_q}| \sum_{n=1}^{N_T} x_n - \sum_{n \neq n_q}^{N_T} \epsilon_n x_n \leq |v_{n_q}| P_q/c, \end{aligned} \quad (13)$$

 where the last inequality follows because $\sum_{n=1}^{N_T} x_n \leq P_q/c$ and $\sum_{n \neq n_q}^{N_T} \epsilon_n x_n \geq 0$. Finally, the proof follows because the solution in (12) achieves the upper-bound in (13). ■

 2) *Optimization of \mathbf{w}* : Defining $\mathbf{u}^H = \mathbf{G} \Phi \mathbf{H} \mathbf{q}$ and noting that the optimal phases of the entries of \mathbf{w} need to fulfill the identity $\angle w_n = \angle u_n$, the problem to be solved reduces to

$$\max_{\mathbf{y}} \sum_{n=1}^{N_T} |u_n| y_n \quad (14a)$$

$$\text{s.t.} \sum_{n=1}^{N_T} y_n \leq P_w/d, y_n \geq 0, \forall n \quad (14b)$$

 with $y_n = |w_n|$ for $n = 1, \dots, N_T$. The following result holds.

Proposition 2: Denote by $n_w \in \{1, 2, \dots, N_T\}$ the index such that $|u_{n_w}| \geq |u_n|$, for $n = 1, \dots, N_T$. Then, the optimal solution of Problem (14) is given by

$$\begin{cases} y_n = \frac{P_w}{d}, & \text{for } n = n_w \\ y_n = 0, & \text{for } n \neq n_w \end{cases} \quad (15)$$

The proof follows along the same line of reasoning as for the proof of Proposition 1 and it is hence omitted.

Algorithm 2 Alternating maximization of Problem (10a) with $P_q/c \leq 1$ and $P_w/d \leq 1$.

Initialize \mathbf{w} and \mathbf{q} to feasible values.
repeat
 $\mathbf{g} = \mathbf{w}^H \mathbf{G}; \mathbf{h} = \mathbf{H}\mathbf{q}; \phi_n = -\angle g_n^* h_n, \forall n = 1, \dots, N;$
 $\mathbf{v}^H = \mathbf{w}^H \mathbf{G}\Phi\mathbf{H}; q_{n_q} = \frac{P_q}{c} e^{j\angle v_{n_q}}, q_n = 0, \forall n \neq n_q;$
 $\mathbf{u} = \mathbf{G}\Phi\mathbf{H}\mathbf{q}; w_{n_w} = \frac{P_w}{d} e^{j\angle u_{n_w}}, w_n = 0, \forall n \neq n_w;$
until Convergence

In the special case considered in this subsection, therefore, Algorithm 1 simplifies to Algorithm 2. The complexity of Algorithm 2 is of the order of $\mathcal{O}(INN_T N_R)$, due to the computation of ϕ_n , \mathbf{v} , and \mathbf{u} in each iteration, and to the number I of iterations until convergence.

C. Joint Optimization of \mathbf{q} , \mathbf{w} , Φ

Based on the insights gained by developing Algorithm 2, it is possible, always assuming $P_q/c \leq 1$ and $P_w/d \leq 1$, to obtain the optimal solution of Problem (7) when \mathbf{q} , \mathbf{w} , Φ are jointly optimized. By direct inspection of Proposition 1 and Proposition 2, in fact, we evince that the optimal \mathbf{q} and \mathbf{w} have only one non-zero component, namely they can be written as

$$\mathbf{q} = \frac{P_q}{c} e^{j\phi_q(\Phi, \mathbf{w})} \underbrace{[0, \dots, 0, 1, 0, \dots, 0]}_{n_q-1} \quad (16)$$

$$\mathbf{w} = \frac{P_w}{d} e^{j\phi_w(\Phi, \mathbf{q})} \underbrace{[0, \dots, 0, 1, 0, \dots, 0]}_{n_w-1}, \quad (17)$$

where we have highlighted the fact that the optimal ϕ_q will depend on Φ and \mathbf{w} through the vector \mathbf{v} , and that the optimal ϕ_w will depend on Φ and \mathbf{q} , through the vector \mathbf{u} .

In practice, (16) and (17) imply that, under the assumption of isotropic EMF constraints, the optimal solutions for the transmit beamforming and the receive decoding vectors consist of activating a single antenna at the transmitter and a single antenna at the receiver, which need to be appropriately chosen. In this section, therefore, we seek for optimal solutions of the form given in (16) and (17).

By plugging (16) and (17) into (10a), we obtain

$$|\mathbf{w}^H \mathbf{G}\Phi\mathbf{H}\mathbf{q}| = \left| \frac{P_q}{c} \frac{P_w}{d} e^{j\phi_q(\Phi, \mathbf{w})} e^{-j\phi_w(\Phi, \mathbf{q})} \mathbf{g}_{n_w}^T \Phi \mathbf{h}_{n_q} \right| =$$

$$\frac{P_q}{c} \frac{P_w}{d} |\mathbf{g}_{n_w}^T \Phi \mathbf{h}_{n_q}| \leq \frac{P_q}{c} \frac{P_w}{d} \sum_{n=1}^N |g_{n_w}(n) h_{n_q}(n)|, \quad (18)$$

wherein $\mathbf{g}_{n_w}^T$ is the n_w -th row of \mathbf{G} , \mathbf{h}_{n_q} is the n_q -th column of \mathbf{H} , and the last inequality is obtained with equality upon optimizing Φ , i.e., by choosing $\phi_n = -\angle g_{n_w}(n) h_{n_q}(n)$ for $n = 1, \dots, N$, with $g_{n_w}(n)$ and $h_{n_q}(n)$ being the n -th components of \mathbf{g}_{n_w} and \mathbf{h}_{n_q} .

Thus, the phases $\phi_q(\Phi, \mathbf{w})$ and $\phi_w(\Phi, \mathbf{q})$ do not affect the value of the objective function, regardless of the values of \mathbf{q} , \mathbf{w} , Φ . Therefore, the last variables that remain to be optimized are the indexes n_w and n_q , which is difficult to be performed in closed-form but can be obtained through an exhaustive search

Algorithm 3 Global optimization of Problem (7) with $P_q/c \leq 1$ and $P_w/d \leq 1$.

for $i = 1$ **to** N_T **do**
for $j = 1$ **to** N_R **do**
 $n_q = i; n_w = j; \text{Obj}(i, j) = \sum_{n=1}^N |g_{n_w}(n) h_{n_q}(n)|;$
end for
end for
 $(n_w^o, n_q^o) = \text{argmax Obj}(i, j);$
 $\mathbf{q} = \frac{P_q}{c} \underbrace{[0, \dots, 0, 1, 0, \dots, 0]}_{n_q^o-1}; \mathbf{w} = \frac{P_w}{d} \underbrace{[0, \dots, 0, 1, 0, \dots, 0]}_{n_w^o-1};$
 $\phi_n = -\angle g_{n_w^o}(n) h_{n_q^o}(n).$

over all possible $N_T N_R$ choices of the pair (n_w, n_q) . This leads to the optimization procedure described in Algorithm 3, which computes (18) for each choice (n_w, n_q) , selects the choice (n_w^o, n_q^o) that yields the largest value of (18), and then allocates the system resources accordingly.

The complexity of Algorithm 3 is $\mathcal{O}(N N_T N_R)$, because the variable $\text{Obj}(i, j)$ needs to be computed $N_T N_R$ times, and each computation requires N complex multiplications.

IV. NUMERICAL RESULTS

In this section, we illustrate some numerical results to assess the benefits of deploying RISs in SAR-constrained wireless networks, so as to enhance the data rate and to simultaneously reduce the EMF exposure of the end-users. We set $B = 5$ MHz, $\delta = 110$ dB, $N_0 = -174$ dBm/Hz, $N_T = N_R = 4$. As for the fading channels, a Rician model is considered, wherein $h_n \sim \mathcal{CN}(v_h, 1)$ and $g_n \sim \mathcal{CN}(v_g, 1)$, with v_h and v_g such that the power of the line-of-sight path is four times larger than the power of all the other paths. All results are averaged over 10^3 independent realizations of the channel vectors \mathbf{h} and \mathbf{g} . The SAR coefficients are set to $c_n = c = 1/N_T$, and $d_n = d = 1/N_R$. For simplicity, thus, we consider the isotropic EMF setup.

Figures 2 and 3 show the system achievable rate and the EMF exposure¹ $c \sum_{n=1}^N |q_n|$, respectively, as a function of P_q/c for $N = 100$, and as a function of N for $P_q/c = 0.85$. The following schemes are considered and evaluated:

- The EMF-aware alternating optimization of \mathbf{q} , \mathbf{w} , and Φ by using Algorithm 1.
- The EMF-aware globally optimal optimization of \mathbf{q} , \mathbf{w} , and Φ , by using Algorithm 3. In this case, the curve is shown only in the range $P_q/c \leq 1$, since beyond this value the assumptions in Section III-B1 do not hold.
- The EMF-aware alternating optimization of \mathbf{q} and \mathbf{w} by using Algorithm 1. In this case, the RIS matrix Φ is not optimized and each RIS phase shift is randomly set in the range $[0, 2\pi]$.
- The EMF-aware globally optimal optimization of \mathbf{q} and \mathbf{w} , by using Algorithm 3. Also in this case, each RIS phase shift is randomly set in the range $[0, 2\pi]$. Moreover, this curve is shown in the range $P_q/c \leq 1$, since beyond this value the assumptions in Section III-B1 do not hold.
- The EMF-unaware optimization of \mathbf{q} , \mathbf{w} , and Φ by using the alternating optimization method from [4].

¹We focus on the exposure due to the transmit antennas. Similar results hold for the EMF exposure due to the receive antennas.

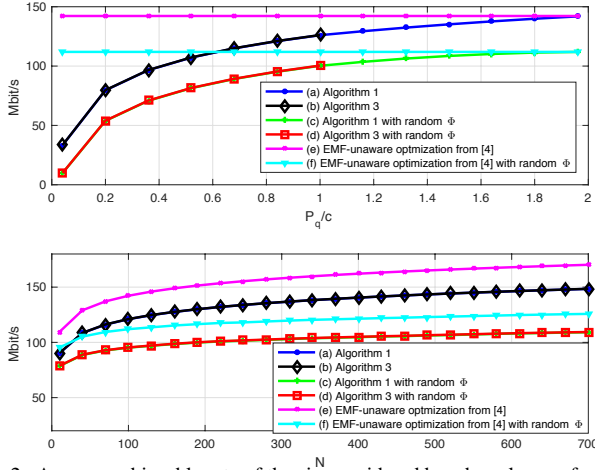


Fig. 2. Average achievable rate of the six considered benchmarks as a function of (top) P_q/c for $N = 100$ and (bottom) N for $P_q/c = 0.85$.

(f) The EMF-unaware optimization of \mathbf{q} and \mathbf{w} , by using the alternating optimization method from [4]. In this case, each RIS phase shift is randomly set in the range $[0, 2\pi]$.

From Figs. 2 and 3, we observe that, in general, enforcing an EMF constraint on the SAR of the human body reduces the achievable rate. The use of RISs offers, however, the opportunity for achieving the desired data rate while ensuring SAR-compliant communications. Figure 2 shows, in particular, that, by increasing N , we can attain the same rate as the benchmark systems in the absence of EMF constraints. EMF-aware transmission schemes lead, on the other hand, to large values of the EMF exposure $c \sum_{n=1}^N |q_n|$ (i.e., the EMF exposure), which may not fulfill the desired SAR values specified by national and international communications commissions. It is particularly interesting to note in Figure 3 that increasing N has little or no impact on the EMF exposure $c \sum_{n=1}^N |q_n|$ imposed to the transmit beamforming and receive decoding vectors. Also, we observe that Algorithm 1 offers similar performance as the globally optimal solution obtained with Algorithm 3, and that, as expected, the SAR-constrained rate tends, for large values of P_q/c , to the benchmark rate in the absence of EMF constraints. This is because increasing P_q/c makes the EMF constraint become less relevant.

By combining the results in Figs. 2 and 3, we conclude that, in RIS-assisted systems, we can enforce the desired EMF constraints while achieving the desired data rate by simply increasing the size of the RIS (i.e., N). In other words, an RIS allows us to keep under control the near-field EMF exposure (i.e., the SAR constraint) while ensuring the desired wireless communication system far-field performance. Notably, this is obtained by using nearly-passive RISs that do not increase the amount of electromagnetic radiation over the air.

V. CONCLUSIONS

In this paper, we have shown how an RIS can be utilized for providing high data rate communications while, at the same time, fulfilling EMF exposure constraints. Low-complexity optimization algorithms have been proposed, which are proved to enjoy global optimality in the special case of isotropic EMF constraints. The numerical results have shown that RISs are

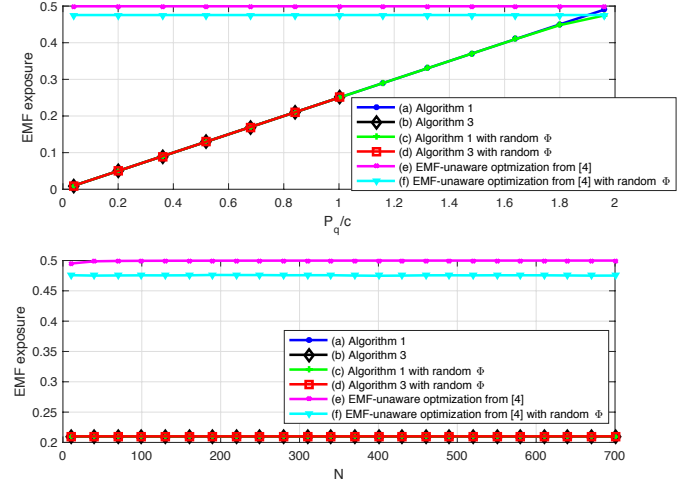


Fig. 3. EMF constraint $c \sum_{n=1}^N |q_n|$ of the six considered benchmarks as a function of (top) P_q/c for $N = 100$ and (bottom) N for $P_q/c = 0.85$.

able to meet the EMF constraints imposed by regulatory bodies while providing satisfactory data rates, in agreement with the demands of future wireless communication networks.

REFERENCES

- [1] M. Di Renzo *et al.*, “Smart radio environments empowered by reconfigurable intelligent surfaces: How it works, state of research, and the road ahead,” *IEEE J. Sel. Areas Commun.*, vol. 38, no. 11, pp. 2450–2525, Nov. 2020.
- [2] Q. Wu and R. Zhang, “Towards smart and reconfigurable environment: Intelligent reflecting surface aided wireless network,” *IEEE Commun. Mag.*, vol. 58, no. 1, pp. 106–112, Jan. 2020.
- [3] M. Di Renzo *et al.*, “Smart radio environments empowered by reconfigurable AI meta-surfaces: An idea whose time has come,” *EURASIP J. Wireless Commun. Netw.*, vol. 129, 2019.
- [4] A. Zappone *et al.*, “Overhead-aware design of reconfigurable intelligent surfaces in smart radio environments,” *IEEE Trans. Wireless Commun.*, vol. 20, no. 1, pp. 126–141, January 2021.
- [5] C. Pan *et al.*, “Multicell MIMO communications relying on intelligent reflecting surface,” *IEEE Trans. Wireless Commun.*, vol. 19, no. 8, pp. 5218–5233, Aug. 2020.
- [6] Q. Wu and R. Zhang, “Intelligent reflecting surface enhanced wireless network: Joint active and passive beamforming design,” *IEEE Trans. Wireless Commun.*, vol. 18, no. 11, pp. 5394–5409, Nov. 2019.
- [7] C. Huang *et al.*, “Reconfigurable intelligent surfaces for energy efficiency in wireless communication,” *IEEE Trans. Wireless Commun.*, vol. 18, no. 8, pp. 4157–4170, Aug. 2019.
- [8] International Commission on Non-Ionizing Radiation Protection, “IC-NIRP guidelines on limiting the exposure to time-varying electric, magnetic and electromagnetic fields (100kHz to 300 GHz),” 2018.
- [9] L. Chiaraviglio, A. Elzanaty, and M. Alouini, “Health risks associated with 5G exposure: A view from the communication engineering perspective,” Available: <https://arxiv.org/abs/2006.00944>, 2020.
- [10] Y. Sambo, F. Heliot, and M. A. Imran, “A survey and tutorial of electromagnetic radiation and reduction in mobile communication systems,” *IEEE Commun. Surv. Tutor.*, vol. 17, no. 2, pp. 790–802, 2015.
- [11] M. Wang *et al.*, “Evaluation and optimization of the specific absorption rate for multiantenna systems,” *IEEE Trans. Electromagn. Compat.*, vol. 53, no. 3, pp. 628–637, Aug. 2011.
- [12] Y. Sambo, M. Al-Imari, F. Heliot, and M. Imran, “Electromagnetic emission-aware schedulers for the uplink of OFDM wireless communication systems,” *IEEE Trans. Vehic. Technol.*, vol. 66, no. 2, pp. 1313–1323, Feb. 2017.
- [13] M. R. Castellano *et al.*, “Dynamic electromagnetic exposure allocation for Rayleigh fading MIMO channels,” *IEEE Trans. Wireless Commun.*, vol. 20, no. 2, pp. 728–740, Feb. 2021.
- [14] H. Ibraiwish, A. Elzanaty, Y. Al-Baderneh, and M. Alouini, “EMF-aware cellular networks in RIS-assisted environments,” Available: <https://repository.kaust.edu.sa/handle/10754/666963>, 2021.